



**HAL**  
open science

# Pre-compensation of thermally induced refractive index changes in a depressed core Fully-Aperiodic Large-Pitch-Fiber for high average power operation

Marie-Alicia Malleville, Baptiste Leconte, Romain Dauliat, Raphaël Jamier, Anka Schwuchow, Katrin Wondraczek, Philippe ROY

## ► To cite this version:

Marie-Alicia Malleville, Baptiste Leconte, Romain Dauliat, Raphaël Jamier, Anka Schwuchow, et al.. Pre-compensation of thermally induced refractive index changes in a depressed core Fully-Aperiodic Large-Pitch-Fiber for high average power operation. *Optics Letters*, 2021, 10.1364/OL.424743 . hal-03857919

**HAL Id: hal-03857919**

**<https://hal.science/hal-03857919>**

Submitted on 17 Nov 2022

**HAL** is a multi-disciplinary open access archive for the deposit and dissemination of scientific research documents, whether they are published or not. The documents may come from teaching and research institutions in France or abroad, or from public or private research centers.

L'archive ouverte pluridisciplinaire **HAL**, est destinée au dépôt et à la diffusion de documents scientifiques de niveau recherche, publiés ou non, émanant des établissements d'enseignement et de recherche français ou étrangers, des laboratoires publics ou privés.

# Pre-compensation of thermally induced refractive index changes in a depressed core Fully-Aperiodic Large-Pitch-Fiber for high average power operation

MARIE-ALICIA MALLEVILLE,<sup>1,2,\*</sup> BAPTISTE LECONTE,<sup>1</sup> ROMAIN DAULIAT,<sup>1,3</sup>  
RAPHAËL JAMIER,<sup>1</sup> ANKA SCHWUCHOW,<sup>3</sup> KATRIN WONDRAKZEK,<sup>3</sup> AND PHILIPPE  
ROY<sup>1</sup>

<sup>1</sup>University of Limoges, CNRS, XLIM, UMR 7252, F-87000 Limoges, France

<sup>2</sup>Eolite Systems, 11 Avenue de Canteranne, 33600 Pessac, France

<sup>3</sup>Leibniz Institute of Photonic Technology, Albert-Einstein-Straße 9, 07745 Jena, Germany

\*Corresponding author: marie-alicia.malleville@xlim.fr

Received XX Month XXXX; revised XX Month, XXXX; accepted XX Month XXXX; posted XX Month XXXX (Doc. ID XXXXX); published XX Month XXXX

**To prevent the thermally induced spatial beam degradation occurring in high-power fibre lasers and amplifiers, a depressed core “Fully Aperiodic Large-Pitch Fibers” (FA-LPFs) has been designed and fabricated. In contrast to standard LPF structure, in which the active core and the surrounding cladding material are index-matched, the core refractive index is in slight depression comparing to the surrounding material ( $\Delta n \approx -3 \times 10^{-5}$ ). Thus, the index-depressed fibre core tends first to behave as an anti-guide, preventing light from being properly guided into it. However, by increasing the pump power coupled in the fiber, the thermal load induces a parabolic refractive index change sufficient to exceed the  $-3 \times 10^{-5}$  index depression in the core, enabling a robust single-mode amplification at high average power. As a proof of concept,  $M^2$  values of 1.3 were demonstrated in an amplifier configuration from 60 W of emitted power to a maximal value of 170 W only limited by the available pump power.**

**OCIS codes:** (060.4005) Microstructured fibers; (060.2430) Fibers, single-mode; (140.3510) Lasers, fiber.

Since the development of Photonic Crystal Fibers (PCF) by Knight et al. [1], numerous microstructured Very-Large-Mode-Areas (VLMA) optical fibers, such as Distributed Mode Filtering (DMF) fibers [2] and Large-Pitch Fibers (LPFs) [3], have been designed for power scaling fiber lasers and amplifiers. These fibers concepts, which can stand the propagation of a very large mode areas beam while maintaining a transverse single-mode operation, have set state-of-the-art performances in terms of core diameters, pulse energy, average and peak power. For instance, a 25 ps mode-locked seed laser was amplified up to 314 kW and 314 W of peak and average power respectively using a DMF fiber whose mode field diameter (MFD) attained 60  $\mu\text{m}$  [4]. Further average power scaling in amplifiers based on a single microstructured fiber has been mainly limited by the onset of transverse mode instabilities (TMI) [5], a threshold-like phenomenon resulting in a significant degradation of the fiber laser beam quality. This phenomenon, originally from the quantum defect of rare-earth ions doped gain media as well as the photodarkening, yields into a heat deposition throughout the fiber. This thermal load induces a transverse parabolic evolution of the core refractive index steadily reconfining High-Order Modes (HOM) into the gain region, leading to an unexpected modal beating and a multimode fashion [5]. One way of circumventing this issue consists in coherently

combining fiber amplifiers delivering peak/average powers many times higher than that achievable with a single amplifier. Thus, pulse energies and peak powers of 5.7 mJ and 22 GW, respectively, have been attained by coherently combining four parallel LPFs amplifiers. These performances were demonstrated in a chirped-pulse amplifier providing a compressed average power of 230 W [6]. Another relevant approach relies on the development of new VLMA fiber designs allowing a further increase of the average power limit. Interesting works have been achieved for instance on thermally guiding index-antiguinding VLMA fibers (TG-IAG) [7,8] in which the core refractive index is set lower than that of the cladding, in order to reduce the impact of thermal load on the transverse index gradient. Thus, the additional mismatch between the core and the cladding generated by the accumulation of heat load throughout the fiber could be reduced. Jansen et al. demonstrated that even if step-index fibers with a small index step or a depressed core improve the beam quality compared to standard step-index fibers; such a design will inevitably leads to multimode operation at high power while more complex designs based on the modal sieve concept would exhibit a transverse single-mode emission.

In this context, authors proposed an original design known as Fully-Aperiodic Large-Pitch Fibers (FA-LPF) [9]. This fiber geometry, relying on the modal sieve concept [10] applied to an aperiodic cladding lattice, exacerbates the delocalization of high-order modes out of the active core. Single-mode operation at  $1\ \mu\text{m}$  was obtained for both passive [9] and active FA-LPF (used as active fiber laser) [11,12,13] with core diameters higher than  $70\ \mu\text{m}$ . For both fibers, materials were fabricated using the REPUSIL manufacturing method owing to its high degree of control over the refractive index value ( $\leq 10^{-4}$ ) [12,14]. Firstly, in this paper, a numerical study was conducted in order to compare the beam quality achieved with two FA-LPF designs: one with a perfect index-matching ( $\Delta n=0$ ) and the other one with an index-depressed core ( $\Delta n<0$ ) regarding the thermal load [15] and, secondly, an experimental work has also been implementing to complete our numerical calculations. The objective here is to show that a FA-LPF with a depressed-core enables to overcome the previous average power limit reached with a FA-LPF with a small index step [12,13].

Based on the numerical investigation performed in [15] using a finite element commercial software, an active depressed-core FA-LPF, schematically represented in Fig.1, has been devised. On one hand, the original aperiodic disposition of solid low-index inclusions - in yellow in Fig.1 - into the passive high-index cladding - in clear blue in Fig.1 - contributes to the confinement of the  $LP_{01}$  mode into the actively doped core - in red in Fig.1 - while exacerbating the HOMs delocalization out of it [9]. On the other hand, the core material does not satisfy anymore the index-matching condition between the active core and the passive cladding by privileging instead a slight core index-depression of  $\Delta n = -3.10^{-5}$ , as represented in Fig.1(b). Thereby, the amplification of the  $LP_{01}$  core mode will be prevented at low power but once the heat load will be sufficient to compensate the refractive index depression, an

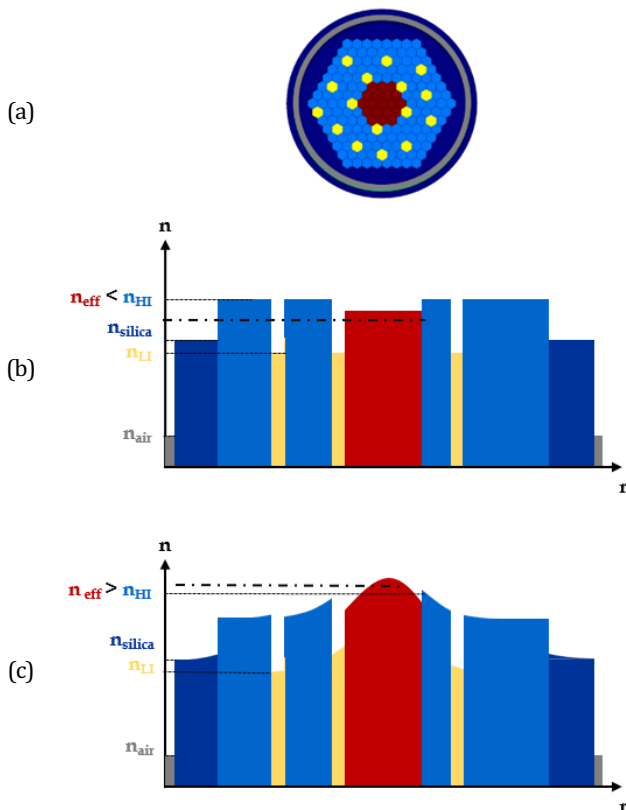


Fig. 1. Schematic representation of a depressed-core ( $n_{\text{core}} < n_{\text{HI}}$ ) FA-LPF refractive index (a) mapping, (b) profile for a “cold fiber” and (c) profile under thermal load. Red and clear blue areas represent respectively the Yb-doped core ( $n_{\text{core}}$ ) and the passive high-index cladding background material ( $n_{\text{core}} < n_{\text{HI}}$  here in contrast to  $n_{\text{core}} = n_{\text{HI}}$  in standard FA-LPF). Low-index inclusions stand as yellow areas ( $n_{\text{BI}} < n_{\text{silica}}$ ). The pure silica is in navy while the pump cladding is in grey. The effective index  $n_{\text{eff}}$  of the  $LP_{01}$  core mode is represented by the dashed and dotted black line.

effective amplification of the  $LP_{01}$  will be retrieved. Indeed, when such fiber will be used as laser or amplifier, a heat load proportional to the amount of non-radiated pump photons, i.e. the quantum defect and the photo-darkening, will be deposited throughout the fiber section and length. Consequently, through a thermo-optic process, the refractive index profile will adopt a parabolic shape across the actively doped core and decay logarithmically into the cladding as represented in Fig.1 (c), contributing to the re-confinement of modes into the active core. Fig. 2 and Fig. 3 give an insight on the dynamic of modes re-confinement at an operating wavelength of  $1030\ \text{nm}$  into both an index-matched ( $\Delta n=0$ ) and an index-depressed core ( $\Delta n=-3.10^{-5}$ ) FA-LPF whose core diameter is arbitrarily set to  $105\ \mu\text{m}$ .

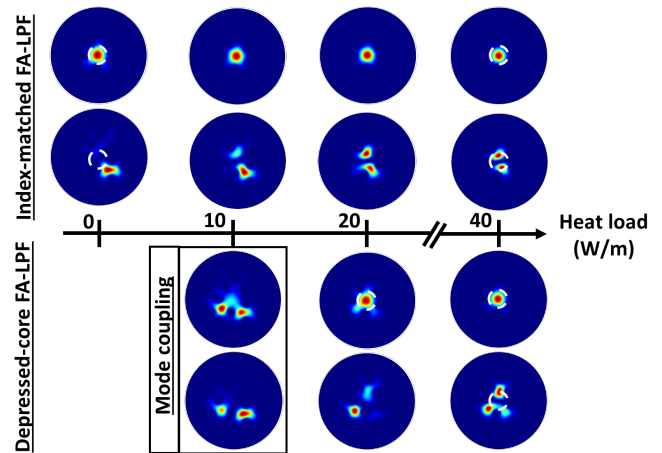


Fig. 2. Computed intensity distributions at an operating wavelength of  $1030\ \text{nm}$  for the first two guided modes into  $105\ \mu\text{m}$  index-matched ( $\Delta n=0$ ) and index-depressed ( $\Delta n=-3.10^{-5}$ ) core FA-LPF, respectively on the top half and bottom half of the figure, versus the heat load. The white dashed rings delimit the actively doped region.

As stated above and seen on the top half of Fig. 2, an index-matched FA-LPF assures a proper confinement of  $LP_{01}$  into the core region while effectively delocalizing HOM out of it. In fact, the “ $LP_{11}$  mode” is for low heat load values identified as a cladding mode since its overlap factor  $\Gamma_{11}$  does not exceed 30%. Then, by steadily rising the heat load toward  $40\ \text{W/m}$ , both modes become confined into the core: the MFD of the  $LP_{01}$  mode shrinks from  $86.3$  to  $70.2\ \mu\text{m}$  while the  $LP_{11}$  mode overlap factor sufficiently rises, yielding into a modal discrimination less than 30% above  $20\ \text{W/m}$ , i.e. a multimode operation.

In contrast, a depressed core FA-LPF prevents the re-confinement of HOMs into the actively doped core and shifts the single-mode regime toward higher heat load, and so, higher average power. As it can be seen on the computed intensity distributions shown on the bottom half of Fig. 2, the FM of such a structure is at first not guided in the fiber core. Owing to the core index depression, the effective index  $n_{\text{eff}}$  of the  $LP_{01}$  core mode is close to that of many cladding modes. Under this circumstance, the  $LP_{01}$  core mode experiences multiple mode coupling with cladding modes, yielding in a significant beam degradation as seen on Fig. 2. This index depression over the whole core cross section is even more detrimental to the HOMs existence in the core, meaning HOMs are even less likely to be effectively amplified than the FM. However, the heat load deposited across the active fiber core gradually induces a quadratic refractive index modification across the fiber core section (Fig 1(c)). This way, the  $LP_{01}$  mode effective index  $n_{\text{eff}}$  increases until standing out from all cladding modes effective indices, as depicted on Fig 1(c), avoiding any mode coupling. The overlap of the  $LP_{01}$  core mode with the actively doped core steadily rises, resulting in an effective confinement of the  $LP_{01}$

mode into the gain region ( $\Gamma_{FM} > 80\%$ ) and to an efficient single-mode amplification for a heat load ranging from 23 W/m to 55 W/m at least as it can be seen on Fig.2 and Fig.3. Over this heat load range, the MFD spans from 92 to 75.7  $\mu\text{m}$ . This not only proves a shift of the operating heat load range of operation due to the index-depression of the active core but also larger MFD than that available into the original FA-LPF structure.

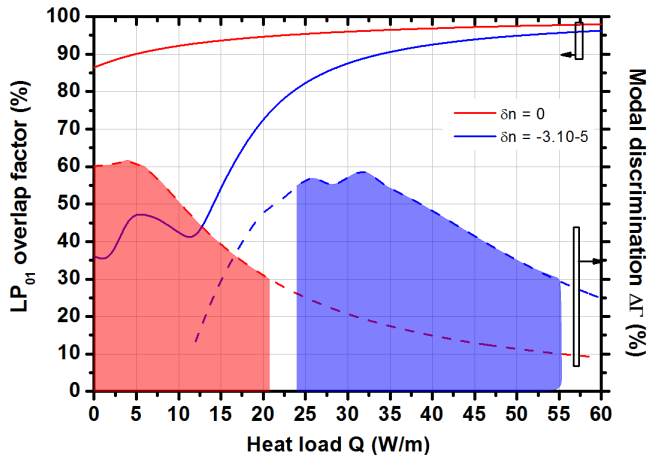


Fig. 3. Evolution of the fundamental  $LP_{01}$  mode overlap factor (solid lines) and modal discrimination (dashed lines) as a function of the heat load “Q” at an operating wavelength of 1030 nm. Two FA-LPF are considered: one with a perfect index-matching between the active core and the background cladding material (red curves –  $\Delta n = 0$ ) and a second with a depressed core (blue curve –  $\Delta n = -3.10^{-5}$ ). Red and blue filled-up areas represent the range over which the single-mode criteria are satisfied:  $\Gamma_{01} > 80\%$  and  $\Delta\Gamma > 30\%$ .

A specific index-depressed FA-LPF design pre-compensating the thermal-induced refractive index changes has thus been drawn. The active and passive materials, prepared using the REPUSIL synthesis technique, show a refractive index contrast  $\Delta n$  of  $-3 \times 10^{-5}$ . This quantity was measured following the methodology described in [16], which offers a resolution of  $\pm 1.10^{-5}$ . The manufactured depressed-core rod-type FA-LPF, depicted in insert of Fig.4, has been characterized in the nanosecond amplification regime. The experimental setup, represented in Fig. 4, is a master oscillator power fiber amplifier system. The seed source delivers 12 ns pulses at 1030 nm at an average power up to 5 W of average power and a repetition rate of 250 kHz.  $M_3$ ,  $M_4$  and  $M_5$  are high-reflectivity mirrors at 1030 nm and  $L_3$  is used to launch the signal power at 1030 nm coming from the seeder into the fiber core with a special care for the mode-matching. The amplifier is based on an 85-cm long rod-type fiber whose MFD is estimated at 92  $\mu\text{m}$  at a low power level. Both fiber end facets were angle-polished at  $5^\circ$  in order to prevent any parasitic reflections and therefore any laser effect. The fiber air clad diameter is 390  $\mu\text{m}$ . This main amplifier is pumped in the counter-propagative direction through the couple of lenses  $L_1$  and  $L_2$  by a 400W – 400  $\mu\text{m}$  – NA 0.22 diode centered at 976 nm at full power. After amplification, the mirror  $M_1$  separates the signal from the pump while the  $M_2$  prevents an optical feedback at 976 nm from damaging the seeder. Thus, the output signal is monitored using a power-meter and its far-field intensity distribution is imaged on a CCD camera thanks to  $L_4$  lens and a set of wedge plates ( $W_1$  and  $W_2$ ). Finally, the  $M^2$  parameter was also measured and a photodiode was employed to investigate the TMI temporal behavior.

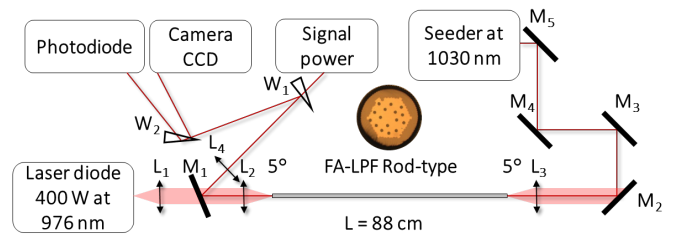


Fig. 4. Schematic representation of the experimental amplifier setup.  $M_1$ , and  $M_2$  are dichroic mirrors (HR1030/HT976);  $M_3$ ,  $M_4$ ,  $M_5$  are HR mirrors at 1030 nm;  $L_1$ ,  $L_2$ ,  $L_3$ , and  $L_4$  are AR-coated lenses and  $W_1$  and  $W_2$  are wedge plates. Insert: microscope image of the depressed-core FA-LPF.

The evolution of the emitted power as a function of the incident pump power is reported in Fig. 5. Two different operating regimes can be identified. Below 200 W of pump power, the FM strongly leaks in the surrounding cladding due to coupling with cladding modes as shown on the near-field intensity distributions of Fig.5. Since the FM weakly overlaps the gain region, it experiences an ineffective amplification, resulting in a very low optical-to-optical efficiency ranging from 15 % to 37 % respectively for 0.4 W and 5 W of seed power. In the second regime, so for pump power values strictly higher than 200 W, the FM overlap with the gain region becomes sufficient to allow an efficient amplification of the single fundamental mode, yielding into optical-to-optical efficiency of 28 % and 56 % for respectively 0.4 W and 4.9 W of seed power. The measured  $M^2$  values for a seed power of 5 W varied from 1.3 at 220 W of pump power to 1.2 at the maximal pump power level. The maximal extracted signal power was of 170W. It is worth noticing that the saturation regime was reached for seed power exceeding 2.8W since the extracted signal power remained from this point unchanged although the seed power was increased. No TMI were observed using the same measurement protocol as in [11,12,15] despite the large core size (105  $\mu\text{m}$ ), meaning that the signal was pump power limited.

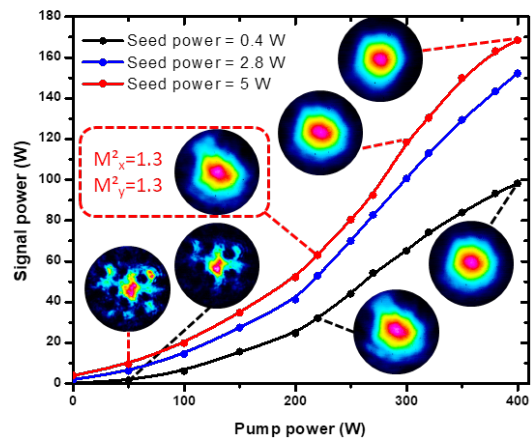


Fig. 5. Evolution of the emitted signal power versus incident pump power for three seed power levels (0.4, 2.8, and 5 W). Inserts depict the far-field intensity distribution for the 92- $\mu\text{m}$  MFD fiber at four levels of pump power: 50 W, 200 W, 300 W, 400 W.

In conclusion, an experimental investigation in high-power amplification regime of the re-confinement of the FM in a depressed core FA-LPF with a very large gain area is reported. This study was conducted over a FA-LPF with a 105  $\mu\text{m}$  index-depressed core ( $\Delta n \approx -3 \times 10^{-5}$ ). Two different operation regimes were identified. At first, the FM leaks in the

background cladding for pump power levels lower than 200 W. Then, according to  $M^2$  factor measurements and to the investigation of the temporal behavior of the emitted beam (no TMI power threshold measured), a re-confinement of the  $LP_{01}$  mode is ensured for pump power values strictly higher than 200 W resulting in a higher slope efficiency. We demonstrated for a depressed core FA-LPF that the heat load range for which an effective transverse single-mode operation can be preserved is expanded even for a fiber with a MFD exceeding 75  $\mu\text{m}$  at full power.

**Acknowledgments.** The authors thank the companies involved in the EATLase project (Eolite Systems, Amplitude Systèmes, Thales Optronics SA, Leukos) as well as the region Nouvelle-Aquitaine for supporting this project through a multi-annual collaboration agreement and financial support. We also thank the ANRT for supporting the thesis of M-A. Malleville. Authors also thanks Kay Schuster as ex-leader of the optical fiber team at the IPHT.

## References

1. J. C. Knight, T. A. Birks, P. St. J. Russell, and D. M. Atkin, *Opt. Lett.* **21**, 1547-1549 (1996).
2. T. T. Alkeskjold, M. Laurila, L. Scolari, and J. Broeng, *Opt. Express* **19**(8), 7398-7409 (2011).
3. F. Jansen, F. Stutzki, H-J. Otto, M. Baumgartl, C. Jauregui, J. Limpert, and A. Tünnermann, *Opt. Express* **18**, 26834-26842 (2010).
4. M. Laurila, M. M. Jørgensen, J. Lægsgaard and T. T. Alkeskjold, *IEEE* **978** (2013).
5. Cesar Jauregui, Christoph Stihler, and Jens Limpert, "Transverse mode instability," *Adv. Opt. Photon.* **12**, 429-484 (2020).
6. A. Klenke, S. Hädrich, T. Eidam, J. Rothhardt, M. Kienel, S. Demmler, T. Gottschall, J. Limpert, and A. Tünnermann, *Opt. Lett.* **39**, 6875-6878 (2014).
7. L. Kong, J. Cao, S. Gua, Z. Jiang, and Q. Lu, "Thermal-induced transverse-mode evolution in thermally guiding index-antiguide-core fiber," *Appl. Opt.*, vol. 55, no. 5, pp. 1183-1189 (2016).
8. F. Jansen, F. Stutzki, H. Otto, C. Jauregui, J. Limpert, and A. Tünnermann, "High-power thermally guiding index-antiguide-core fibers," *Opt. Lett.*, vol. 38, no. 4, pp. 510-512, 2013.
9. R. Dauliat *et al.*, "Demonstration of a homogeneous Yb-doped core fully aperiodic large-pitch fiber laser," *Appl. Opt.*, vol. 55, no. 23, 2016.
10. P. St. J. Russell, *Science* **299**, 358 (2003).
11. A. Benoît, R. Dauliat, R. Jamier, G. Humbert, S. Grimm, K. Schuster, F. Salin, and P. Roy, *Opt. Lett.* **39**, 4561-4564 (2014).
12. M-A. Malleville, R. Dauliat, A. Benoît, B. Leconte, D. Darwich, R. du Jeu, R. Jamier, K. Schuster, and P. Roy, *Opt. Lett.* **42**, 5230-5233 (2017).
13. M-A. Malleville, A. Benoît, R. Dauliat, B. Leconte, D. Darwich, R. du Jeu, R. Jamier, A. Schwuchow, K. Schuster, and P. Roy, *Proc. SPIE 10512, Fiber Lasers XV: Technology and Systems*, 1051206 (26 February 2018).
14. K. Schuster, S. Unger, C. Aichele, F. Lindner, S. Grimm, D. Litzkendorf, J. Kobelke, J. Bierlich, K. Wondraczek, and H. Bartelt, *Adv. Opt. Technol.* **3**, 447-468 (2014).
15. D. Darwich, R. Dauliat, R. Jamier, A. Benoit, K. Schuster, and P. Roy, *Appl. Opt.* **55**, 8213-8220 (2016).
16. B. Leconte *et al.*, "Highly resolved interferometric measurement of refractive index difference between two silica-based materials", paper SoTh1H.6, Advanced Photonic Congress 2020 to be published.